

Based on the observations collected with the 6m telescope (BTA) at the Special Astrophysical Observatory (SAO) of the Russian Academy of Sciences (RAS).

Stellar populations in nearby lenticular galaxies

O. K. Sil'chenko

*Sternberg Astronomical Institute, Moscow, 119992 Russia
and Isaac Newton Institute of Chile, Moscow Branch
Electronic mail: olga@sai.msu.su*

ABSTRACT

We have obtained 2D spectral data for a sample of 58 nearby S0 galaxies with the Multi-Pupil Spectrograph of the 6m telescope of the Special Astrophysical Observatory of the Russian Academy of Sciences. The Lick indices $H\beta$, Mgb, and $\langle Fe \rangle$ are calculated separately for the nuclei and for the bulges taken as the rings between $R = 4''$ and $7''$; and the luminosity-weighted ages, metallicities, and Mg/Fe ratios of the stellar populations are estimated by confronting the data to SSP models. Four types of galaxy environments are considered: clusters, centers of groups, other places in groups, and field. The nuclei are found to be on average slightly younger than the bulges in any types of environments, and the bulges of S0s in sparse environments are younger than those in dense environments. The effect can be partly attributed to the well-known age correlation with the stellar velocity dispersion in early-type galaxies (in our sample the galaxies in sparse environments are in average less massive than those in dense environments), but for the most massive S0s, with $\sigma_* = 170 - 220$ km/s, the age dependence on the environment is still significant at the confidence level of 1.5σ .

Subject headings: galaxies: nuclei — galaxies: elliptical and lenticular — galaxies: evolution

1. Introduction

In classical morphological sequence by Hubble (1936) lenticular galaxies occupy intermediate position between ellipticals and spirals: they have a smooth and red appearance

as the ellipticals, but also have stellar disks, almost as large as those of the spirals. The most popular hypothesis of S0 origin is that of their transformation from the spirals by stopping global star formation and removing or consuming remaining gas (Larson et al. 1980). In distant, $z \sim 0.5$, clusters this transformation is now observed directly: the number of lenticulars in the clusters diminishes strongly with the redshift (Fasano et al. 2000), instead one can see ‘passive spirals’ – red spiral galaxies lacking star formation – at the periphery (‘infalling regions’) of the intermediate-redshift clusters (Goto et al. 2003; Yamauchi & Goto 2004). Many theoretical works have been done to explain in detail what physical mechanisms may be involved into the process of spiral transformation into the lenticulars: tidally induced collisions of disk gas clouds (Byrd & Valtonen 1990), harassment (Moore et al. 1996), ram pressure by intercluster medium (Quilis et al. 2000), etc. For the S0s in the field, the scheme of their transformation from the spirals is not so clear, but common view is that some external action like minor merger may produce the necessary effect.

By reviewing the various mechanisms of secular evolution which may transform a spiral galaxy into a lenticular one we have noticed that most of them result in gas concentration in the very center of the galaxy, so that a nuclear star formation burst seems unavoidable circumstance of the S0 galaxy birth. If to refer to S0 statistics in the clusters located between $z = 0$ and $z \approx 1$, the main epoch of S0 formation is $z \approx 0.4-0.5$, so the nuclear star formation bursts in the nearby S0s must not be older than 5 Gyr. Indeed, in my spectral study of the central parts of nearby galaxies in different types of environments (Sil’chenko 1993) I have found that $\sim 50\%$ of nearby lenticulars have strong absorption lines $H\gamma$ and $H\delta$ in their nuclear spectra so they are of ‘E+A’ type, as it is presently called and are dominated by intermediate-age stellar population. In this respect the S0s have resembled rather early-type spirals than ellipticals. Here I aim to continue this study, with a larger sample and with panoramic spectral data in order to separate the nuclei and their outskirts (bulges) which is a substantial advantage with respect to aperture spectroscopy.

Another crucial point of the present study, and also of a global paradigm of galaxy formation, is environmental influence. The current hierarchical assembly paradigm predicts a younger age of galaxies in lower density environments – for the most recent simulations see e.g. Lanzoni et al. (2005) or De Lucia et al. (2005). Observational evidences concerning early-type galaxies are controversial: some authors find differences of stellar population ages between the clusters and the field (Terlevich & Forbes 2002; Kuntschner et al. 2002; Thomas et al. 2005), some authors do not find any dependence of the stellar population age on environment density (Kochanek et al. 2000). In order to check whether the mean ages of the stellar populations depend on environment density monotonously, as the hierarchical paradigm predicts, in this work I consider four types of environments separately: the cluster galaxies, the brightest (central) galaxies of groups, the second-ranked group members, and

the field galaxies.

2. Sample

The sample of lenticular galaxies considered in this work consists of 58 objects, mostly nearby and bright. It does not pretend to be complete but rather representative. In the LEDA we have found 122 galaxies in total with the following parameters: $-3 \leq T \leq 0$, $v_r < 3000$ km/s, $B_T^0 < 13.0$, $\delta_{2000.0} > 0$, without bright AGN or intense present star formation in a nucleus; among them 40 Virgo members. For our sample, from this list we have selected 8 Virgo members and 42 other galaxies – half of the rest. A few galaxies are added to broaden the luminosity range: NGC 5574, NGC 3065, and NGC 7280 are fainter than $B_T^0 = 13.0$, NGC 80 and NGC 2911 are very luminous but farther from us than 40 Mpc.

Table 1. Our sample of S0 galaxies

Galaxy ^a	Environment ^b	Type ^c	σ_0 , km/s ^d	v_r , km/s ^d	Dates (green)	Dates (red)	Detailed description, ref.
N0080	Group center	SA0-	260	5698	Aug96, Oct03	–	Sil’chenko et al. (2003b)
N0474	Pair	(R’)SA(s)0 ⁰	164	2372	Oct03	–	–
N0524	Group center	SA(rs)0+	253	2379	Oct97	Oct96	Sil’chenko (2000)
N0676	Pair	S0/a	140 ^e	1506	Oct03	–	–
N0936	Group center	SB(rs)0+	190	1430	Oct02, Oct03	Oct02	–
N1023	Group center	SB(rs)0-	204	637	Oct96	–	Sil’chenko (1999)
N1161	Pair	S0	185 ^e	1954	Oct03	–	–
N2300	Group member	SA0+	261	1938	Sep01	–	–
N2549	Group center	SA(r)0+	143	1039	Oct04	Oct02	–
N2655	Group center	SAB(s)0/a	163	1404	Oct99, Oct00	Oct00	Sil’chenko & Afanasiev (2004)
N2681	Group center	(R’)SAB(rs)0/a	108	692	Sep01	Mar02	–
N2685	Field	(R)SB0+pec	94	883	Oct94	–	Sil’chenko (1998)
N2732	Pair	S0	154	1960	Oct00	Sep01	Sil’chenko & Afanasiev (2004)
N2768	Group center	S0 _{1/2}	182	1373	Jan01	Oct00	Sil’chenko & Afanasiev (2004)
N2787	Field	SB(r)0+	194	696	Oct00	Oct00	Sil’chenko & Afanasiev (2004)
N2880	Field	SB0-	136	1608	Sep01	–	–
N2911	Group center	SA(s)0:	234	3183	Dec99	Jan98	Sil’chenko & Afanasiev (2004)
N2950	Field	(R)SB(r)0 ⁰	182	1337	Oct03	Oct05	–
N3065	Group center	SA(r)0+	160	2000	Sep01	Oct05	–
N3098	Field	S0	105	1311	Jan01	–	–
N3166	Group member	SAB(rs)0/a	112	1345	Mar03	Jan98	–
N3245	Group member	SA(r)0 ⁰	210	1358	Mar03	–	–
N3384	Group member	SB(s)0-	148	704	Dec99	–	Sil’chenko et al. (2003a)
N3412	Group member	SB(s)0 ⁰	101	841	Mar04	–	–
N3414	Group center	S0pec	237	1414	Jan01	Mar02	Sil’chenko & Afanasiev (2004)
N3607	Group center	SA(s)0+	224	935	Apr01	Mar02	–
N3941	Group center	SB(s)0 ⁰	159	928	Mar03	–	–
N3945	Group member	SB(rs)0+	174	1259	Mar03	–	–
N4026	UMa cluster	S0	178	930	Mar03	–	–
N4036	Group center	S0-	189	1445	May97, Jan98	Jan98	Sil’chenko & Vlasjuk (2001)
N4111	UMa cluster	SA(r)0+	148	807	Jan01	Mar02	Sil’chenko & Afanasiev (2004)
N4125	Group center	E6 pec	227	1356	Mar03	Jan98	–
N4138	UMa cluster	SA(r)0+	140	888	Jan98, Dec99	Dec99	Afanasiev & Sil’chenko (2002)
N4150	Group member	SA(r)0+	85	226	Apr01	Mar02	–
N4179	Group center	S0	157	1256	Mar03	–	–

Table 1—Continued

Galaxy ^a	Environment ^b	Type ^c	σ_0 , km/s ^d	v_r , km/s ^d	Dates (green)	Dates (red)	Detailed description, ref.
N4233	Virgo cluster	S0 ⁰	220	2371	Apr02	Apr02	Sil'chenko & Afanasiev (2004)
N4350	Virgo cluster	SA0	181	1200	Jan01	–	–
N4379	Virgo cluster	S0-	108	1069	Jun99	–	–
N4429	Virgo cluster	SA(r)0+	192	1106	Jun99	May97	Sil'chenko & Afanasiev (2002)
N4526	Virgo cluster	SAB(s)0+	264	448	Apr01	Mar02	–
N4550	Virgo cluster	SB0	91	381	Jan98, Jun99	Jun99	Afanasiev & Sil'chenko (2002)
N4570	Virgo cluster	S0/E7	188	1730	Mar04	–	–
N4638	Virgo cluster	S0-	122	1164	Mar04	–	–
N4866	Pair	SA(r)0+	210	1988	Apr01	–	–
N5308	Group member	S0-	211	2041	Mar03	–	–
N5422	Group member	S0	165	1820	Mar03	–	–
N5574	Group member	SB0-?	75	1659	Jun99	–	Sil'chenko et al. (2002)
N5866	Group member	S0 ₃	159	672	Aug98	May96	–
N6340	Group center	SA(s)0/a	144	1198	Aug96, Oct97	Aug96	Sil'chenko (2000)
N6548	Pair	SB0	121 ^e	2179	Oct04	–	–
N6654	Pair	(R')SB(s)0/a	149 ^e	1821	Sep01	–	–
N6703	Field	SA0-	180	2461	Oct03	Oct03	–
N7013	Field	SA(r)0/a	84	779	Oct96, Aug98	Aug96	Sil'chenko & Afanasiev (2002)
N7280	Field	SAB(r)0+	104	1844	Aug98	Oct98	Afanasiev & Sil'chenko (2000)
N7332	Field	S0 pec	124	1172	Aug96, Oct97	–	Sil'chenko (1999)
N7457	Field	SA(rs)0-?	69	812	Oct99, Dec99	–	Sil'chenko et al. (2002)
N7743	Field	(R)SB(s)0+	84	1710	Oct03	–	–
U11920	Field	SB0/a	116 ^e	1145	Oct03	–	–

^aGalaxy ID – N=NGC, U=UGC

^bFrom Guiricin et al. 2000

^cHubble type from the NED

^dMainly from the LEDA

^eFrom our observations

Table 1 lists all the galaxies with some of their characteristics such as morphological type, redshift, and central velocity dispersion. Sorting of the galaxies according to their environment type has been made by using the NOG group catalogue (Giuricin et al. 2000); we have only classified three galaxies belonging to the Ursa Major cluster following Tully et al. (1996). Our sample includes 11 cluster galaxies, from Virgo and Ursa Major, 17 central (the brightest) galaxies of groups with 3 members and more, 18 second-ranked group members to which we have added paired galaxies, and 12 field lenticulars which are defined as not mentioned in the NOG catalogue at all.

All the galaxies of Table 1 have been observed with the integral-field unit – the Multi-Pupil Fiber/Field Spectrograph (MPFS) ¹ (Afanasiev et al. 2001) of the 6m telescope of the Special Astrophysical Observatory of the Russian Academy of Sciences between 1994 and 2005. For these years the instrument was modified more than once. We started with the field of view of $10'' \times 12''$, with the spatial element (pupil) size of $1''.3$, with the spectral resolution of 5 \AA , and spectral range less than 600 \AA . Now we have $16'' \times 16''$, the spatial element (pupil) size of $1''$, the spectral resolution of 3.5 \AA , and spectral range of 1500 \AA . Usually we observe two spectral ranges, the green one centered onto $\lambda 5000 \text{ \AA}$, and the red one centered onto the $H\alpha$ line. The optical design had been modified too: two different schemes, a TIGER-like one – for the description of the instrumental idea of the TIGER mode of IFU one can see Bacon et al. (1995) – and that with fibers, were used before and after 1998. We have described in detail 23 of 58 lenticulars in our previous papers (see the references in the Table 1) where one can find not only the characteristics of the various versions of the MPFS, but also 2D maps of Lick indices and kinematical parameters. Here we consider only two discrete areas of every galaxy – the unresolved nuclei and the wide rings, with $R_{in} = 4''$ and $R_{out} = 7''$, which we are treating as the ‘bulges’. The boundaries of the rings have been selected as a compromise between the seeing limitation (the seeing FWHM are typically $2''.5$ at the 6m telescope) in order to avoid the influence of the nuclei on the bulge measurements, and the size of our field of view which causes incomplete azimuthal coverage at $R > 7''$. At our limit distance, $D = 40 \text{ Mpc}$, the outer radius of the ‘bulge’ areas, $7''$, corresponds to the linear size of 1.35 kpc . The nuclei are presented by the integrated fluxes over the central spatial elements within the maximum radius of 0.1 kpc from the centers.

¹http://www.sao.ru/hq/lsvfo/devices/mpfs/mpfs_main.html

Table 2: The comparison of two independent index determinations with the MPFS

NGC	$H\beta$, Å		Mgb, Å		$\langle Fe \rangle$, Å	
	nucleus	bulge	nucleus	bulge	nucleus	bulge
80	1.57	1.70	5.12	4.44	3.14	3.22
	1.66	1.59 ± 0.20	5.00	4.44 ± 0.04	2.94	2.95 ± 0.15
936	1.13	1.41 ± 0.03	4.64	4.51 ± 0.03	2.86	2.50 ± 0.01
	1.41	1.07 ± 0.07	4.93	4.53 ± 0.10	3.20	2.80 ± 0.07
2655	1.56	1.55 ± 0.03	3.77	3.60 ± 0.11	2.10	2.07 ± 0.05
	1.73	1.35 ± 0.05	3.70	3.69 ± 0.02	2.38	2.47 ± 0.02
4036	0.12	0.92 ± 0.08	5.56	4.09 ± 0.13	2.56	2.64 ± 0.07
	0.82	0.80 ± 0.08	5.85	3.61 ± 0.25	3.28	–
4138	1.14	1.10 ± 0.03	4.76	3.34 ± 0.15	2.97	2.00 ± 0.14
	0.74	0.96 ± 0.06	4.66	3.45 ± 0.21	2.65	2.11 ± 0.07
4550	1.64	1.92	3.18	3.13	–	–
	1.64	1.41 ± 0.03	3.20	3.14 ± 0.05	2.53	1.95 ± 0.08
6340	1.05	0.86	4.65	3.06	2.92	2.10
	1.56	1.24	4.49	3.18	2.76	2.12
7013	1.63	2.03	3.84	3.32	2.99	–
	1.58	2.15 ± 0.09	3.78	3.27 ± 0.05	3.00	2.35 ± 0.09
7332	2.10	1.54 ± 0.10	3.67	2.54 ± 0.20	2.92	2.05 ± 0.16
	2.24	1.65 ± 0.10	3.80	2.77 ± 0.12	2.80	2.23
7457	1.93	2.27	2.72	3.37	2.49	2.24
	1.99	2.21 ± 0.05	2.92	2.98 ± 0.06	2.44	2.26 ± 0.07

Table 3: The mean differences between our indices and the Trager’s et al. data

	H β	Mgb	$\langle\text{Fe}\rangle$
Δ	+0.07Å	-0.05Å	+0.12Å
	$\pm 0.06\text{\AA}$	$\pm 0.07\text{\AA}$	$\pm 0.09\text{\AA}$

Note. — The second line of the table contains the formal errors of the mean offsets of our index system with respect to the Lick one

The Lick indices $H\beta$, Mgb, Fe5270, and Fe5335 have been measured for the nuclei and for the bulges of all the galaxies; farther we use the composite iron index $\langle Fe \rangle \equiv (Fe5270 + Fe5335)/2$. During all our observational runs we observed standard stars from Worthey et al. (1994) and calibrated our index system onto the standard Lick one. The measured indices were corrected for the stellar velocity dispersions; we calculated the corrections by artificial broadening of the spectra of the standard stars. We estimate the typical statistical accuracy in each of three indices (defined by the S/N ratio which has been kept as 70-90 (per Å) in the nuclei and ~ 30 at the edges of the frames) as 0.1 Å. Some galaxies of the sample have been observed twice. In the Table 2 we show the raw index measurements from two independent observational runs for each of those objects; \pm accompanying the bulge indices reflect partly the index variations along the radii – we average four measurements at four R 's from 4'' to 7'' for each galaxy and give here the errors of the means. The mean absolute difference between two independent index measurements is 0.20 Å for the nuclei and 0.18 Å for the bulges over the Table 2. If we analyse three indices separately, we obtain the mean absolute differences (the rms of the differences) of 0.22 Å (0.29 Å) for $H\beta$, 0.15 Å (0.19 Å) for Mgb, and 0.22 Å (0.28 Å) for the composite iron index. These results mean that the accuracy of the Mgb corresponds to our expectations from the S/N statistics, namely, is 0.1 Å, and the accuracy of the $H\beta$ and $\langle Fe \rangle$ is somewhat worse, namely, is 0.15 Å. Among our 58 galaxies, 28 objects have Lick index measurements through the central aperture $2'' \times 4''$ by Trager et al. (1998). The results of the comparison of these standardized Lick indices with our measurements for the nuclei are presented in Table 3 and in Fig. 1. The smallest scatter is found for $H\beta$ and the largest one – for $\langle Fe \rangle$, that is consistent with the fact that among the four indices, $H\beta$, Mgb, Fe5270, and Fe5335, the errors quoted by Trager et al. (1998) are the smallest for $H\beta$ (0.24 Å on average over the common list) and the largest – for Fe5335 (0.34 Å on average over the common list). In general, our index system does not deviate from the standard Lick one in any systematic way, so we can determine the stellar population properties by confronting our indices to evolutionary synthesis models.

Table 4. Indices and ages for the nuclei of the S0 galaxies

Galaxy ^a	Environment ^b	H β	Mgb	(Fe)	T ^c , Gyr	[Z/H] ^c	EW([OIII]5007), Å	T ^d , Gyr	[Z/H] ^d
N0080	Group center	1.62	5.06	3.04	7	+0.4	0.08	6	+0.5
N0474	Group member (pair)	1.70	4.55	3.14	4	+0.4	0.94	2	$\geq +0.7$
N0524	Group center	1.33	4.87	2.68	14	+0.1	0.46	10	+0.2
N0676	Group member (pair)	1.02	4.16	2.90	> 15	0	2.0	3	+0.7
N0936	Group center	1.27	4.78	3.03	15	+0.2	0.79	5	+0.4
N1023	Group center	1.57	5.03	2.99	8	+0.4	0.12	7	+0.4
N1161	Group member (pair)	1.84	5.31	3.04	3	+0.7	0.06	4	+0.7
N2300	Group member	1.64	5.19	2.87	7	+0.4	0	7	+0.4
N2549	Group center	2.51	4.47	3.32	< 2	$\geq +0.7$	0.20	< 2	$\geq +0.7$
N2655	Group center	1.65	3.74	2.24	2	0	2.51	2	0
N2681	Group center	3.52	2.31	2.02	< 2	≤ 0	0.56	< 2	≤ 0
N2685	Field	1.75	3.59	2.58	4	+0.1	0.57	4	+0.1
N2732	Group member (pair)	1.88	3.55	2.71	7	0	0.46	3	+0.3
N2768	Group center	0.91	4.90	2.64	11	+0.2	0.91	15	+0.1
N2787	Field	0.61	5.25	2.12	> 15	0	0.95	> 15	0
N2880	Field	1.72	4.15	2.63	9	+0.1	0.1	8	+0.2
N2911	Group center	-0.11	5.65	2.59	15	+0.1	2.38	> 15	0
N2950	Field	2.66	4.67	3.23	< 2	$\geq +0.7$	0.28	< 2	$\geq +0.7$
N3065	Group center	0.42	4.16	2.42	- ^e	- ^e	2.36	6	+0.2
N3098	Field	1.79	3.65	2.20	10	-0.2	0.28	7	-0.1
N3166	Group member	2.36	3.68	2.94	< 2	+0.7	0.57	< 2	+0.7
N3245	Group member	0.67	4.52	2.96	6	+0.3	0.61	> 15	+0.1
N3384	Group member	2.04	4.64	3.07	3	+0.7	0.05	3	+0.7
N3412	Group member	2.33	4.00	3.02	2	+0.7	0.23	< 2	+0.7
N3414	Group center	0.82	5.21	2.74	13	+0.2	1.23	7	+0.4
N3607	Group center	0.93	5.24	2.78	12	+0.2	0.71	15	+0.2
N3941	Group center	1.69	4.61	3.26	4	+0.7	0.83	2	$\geq +0.7$
N3945	Group member	1.44	4.74	3.28	6	+0.5	0.30	7	+0.5
N4026	UMa cluster	1.73	4.44	3.11	6	+0.4	0	6	+0.4
N4036	Group center	0.47	5.70	2.92	11	+0.3	1.42	10	+0.4
N4111	UMa cluster	1.99	4.60	2.56	< 2	+0.7	0.54	2	+0.6
N4125	Group center	1.31	4.66	3.14	7	+0.4	0.70	5	+0.5
N4138	UMa cluster	0.94	4.71	2.81	12	+0.2	4.7	< 2	$\geq +0.7$
N4150	Group member	2.65	2.51	1.60	2	-0.2	0.87	< 2	-0.1
N4179	Group center	1.90	4.94	3.31	4	+0.7	0	4	+0.7

Table 4—Continued

Galaxy ^a	Environment ^b	H β	Mgb	$\langle\text{Fe}\rangle$	T ^c , Gyr	[Z/H] ^c	EW([OIII] λ 5007), Å	T' ^d , Gyr	[Z/H] ^d
N4233	Virgo cluster	1.06	4.80	3.00	15	+0.2	0.78	10	+0.3
N4350	Virgo cluster	1.41	5.26	2.91	8	+0.4	0.17	10	+0.4
N4379	Virgo cluster	1.51	4.36	2.45	15	0	0.14	13	0
N4429	Virgo cluster	1.60	4.61	2.96	3	+0.7	0.25	6	+0.4
N4526	Virgo cluster	1.62	4.75	2.78	3	+0.7	0.24	6	+0.4
N4550	Virgo cluster	1.64	3.20	2.53	5	0	1.16	3	+0.2
N4570	Virgo cluster	1.72	5.18	2.86	5	+0.4	0	5	+0.4
N4638	Virgo cluster	2.01	4.75	3.42	3	+0.7	0.06	3	+0.7
N4866	Group member (pair)	1.28	4.60	2.85	8	+0.3	0.69	8	+0.3
N5308	Group member	1.48	5.14	2.92	11	+0.3	0	11	+0.3
N5422	Group member	1.41	4.85	3.28	12	+0.4	0.52	5	+0.5
N5574	Group member	2.78	2.48	2.47	2	0	0.25	< 2	0
N6340	Group center	1.30	4.57	2.84	11	+0.2	0.33	13	+0.2
N6548	Group member (pair)	1.67	4.58	2.90	8	+0.3	0	8	+0.3
N6654	Group member (pair)	1.67	4.51	2.78	8	+0.3	0	8	+0.3
N6703	Field	1.49	4.34	3.14	12	+0.2	0.33	7	+0.3
N7013	Field	1.60	3.81	3.00	6	+0.2	1.08	2	+0.5
N7280	Field	2.61	3.57	3.10	< 2	+0.7	0.07	< 2	+0.7
N7332	Field	2.12	3.72	2.86	3	+0.3	0.25	2	+0.4
N7457	Field	1.96	2.82	2.46	8	-0.2	0.46	4	0
N7743	Field	2.21	3.21	2.26	< 2	+0.7	6.51	< 2	-
U11920	Field	1.60	4.44	3.12	9	+0.3	0.76	3	+0.7

^aGalaxy ID – N=NGC, U=UGC

^bFrom Guiricin et al. 2000

^cEstimated with the H β index corrected from the emission through the equivalent width of H α emission line

^dEstimated with the H β index corrected from the emission through the [OIII] λ 5007 equivalent width

^eWe cannot correct this H β index from the emission through H α equivalent width

Table 5. Indices and ages for the bulges of the S0 galaxies

Galaxy ^a	Environment ^b	H β	Mgb	$\langle\text{Fe}\rangle$	T ^c , Gyr	[Z/H] ^c	EW([OIII]5007), Å	T' ^d , Gyr	[Z/H]' ^d
N0080	Group center	1.60	4.67	2.82	(10)	(+0.2)	0.08	8	+0.3
N0474	Group member (pair)	1.74	4.18	2.99	(7)	(+0.2)	0.35	4	+0.4
N0524	Group center	1.07	3.65	2.00	> 15	0?	0	> 15	0?
N0936	Group center	1.40	4.51	2.50	15	0	0.48	9	+0.2
N1023	Group center	1.43	3.94	2.69	(15)	(-0.1)	0.06	15	-0.1
N1161	Group member (pair)	1.71	4.24	2.86	(8)	(+0.2)	0	8	+0.2
N2300	Group member	1.50	4.85	2.84	(12)	(+0.2)	0	12	+0.2
N2549	Group center	2.22	4.05	3.15	2	+0.7	0.20	2	+0.7
N2655	Group center	1.45	3.64	2.27	15	-0.2	0.78	7	-0.1
N2681	Group center	2.66	2.30	1.97	3	-0.2	0.42	2	-0.2
N2685	Field	1.41	2.63	2.37	(> 15)	(-0.3?)	0.82	9	-0.3
N2732	Group member (pair)	1.62	3.53	2.30	11	-0.2	0.60	6	0
N2768	Group center	1.24	4.21	2.48	13	0	0.70	11	0
N2787	Field	1.03	4.54	2.38	> 15	-0.1?	0.48	> 15	-0.1
N2880	Field	1.74	3.92	2.56	(9)	(0)	0.12	8	+0.1
N2911	Group center	0.69	3.89	2.34	> 15	?	0.78	> 15	< 0
N2950	Field	2.13	4.42	3.02	3	+0.7	0.72	< 2	> +0.7
N3065	Group center	1.54	3.94	2.51	15	-0.1	0.90	4	+0.2
N3098	Field	1.96	3.57	2.33	(6)	(0)	0.32	4	0
N3166	Group member	2.54	3.37	2.66	2	+0.3	0.35	< 2	+0.3
N3245	Group member	1.70	4.30	3.02	(8)	(+0.3)	0.16	5	+0.4
N3384	Group member	1.71	4.00	2.87	(9)	(+0.2)	0.18	7	+0.2
N3412	Group member	2.13	3.62	2.80	(3)	(+0.3)	0.25	2	+0.3
N3414	Group center	1.08	4.70	2.47	15	0	1.05	9	+0.2
N3607	Group center	1.59	4.37	2.83	10	+0.2	0	10	+0.2
N3941	Group center	1.58	3.80	2.70	(13)	(0)	0.87	3	+0.3
N3945	Group member	1.38	4.19	3.12	(15)	(+0.1)	0.12	14	+0.1
N4026	UMa cluster	1.66	4.09	2.89	(10)	(+0.2)	0.59	4	+0.3
N4036	Group center	0.86	3.85	2.64	> 15	?	0.36	> 15	< 0
N4111	UMa cluster	1.61	3.53	2.32	11	-0.2	0.34	6	0
N4125	Group center	1.61	4.64	3.13	6	+0.4	0.34	4	+0.4
N4138	UMa cluster	1.03	3.40	2.06	8	-0.2	1.7	6	-0.1
N4150	Group member	2.22	2.51	1.87	5	-0.3	0.70	3	-0.2
N4179	Group center	1.69	4.35	3.04	(8)	(+0.3)	0	8	+0.3
N4233	Virgo cluster	1.63	4.19	2.78	11	+0.1	0	11	+0.1

Table 5—Continued

Galaxy ^a	Environment ^b	H β	Mgb	$\langle\text{Fe}\rangle$	T ^c , Gyr	[Z/H] ^c	EW([OIII] λ 5007), Å	T' ^d , Gyr	[Z/H] ^d
N4350	Virgo cluster	1.63	4.73	2.75	(9)	(+0.3)	0	9	+0.3
N4379	Virgo cluster	1.66	3.98	2.29	(12)	(-0.1)	0.35	8	0
N4429	Virgo cluster	1.43	4.52	2.69	15	+0.1	0.19	12	+0.1
N4526	Virgo cluster	1.30	4.45	2.76	3	+0.6	0.06	> 15	+0.1
N4550	Virgo cluster	1.66	3.14	1.95	15	-0.3	0.70	6	-0.2
N4570	Virgo cluster	1.64	4.74	2.91	(8)	(+0.3)	0	8	+0.3
N4638	Virgo cluster	2.13	4.17	3.20	(3)	(+0.7)	0	3	+0.7
N4866	Group member (pair)	1.50	4.08	2.23	(15)	(-0.2)	0.60	8	0
N5308	Group member	1.62	4.94	3.04	(7)	(+0.4)	0.08	6	+0.5
N5422	Group member	1.62	4.78	3.16	(7)	(+0.4)	0.73	3	+0.7
N5574	Group member	2.38	3.15	2.43	(3)	(+0.2)	0.36	2	+0.2
N5866	Group member	1.73	3.62	2.95	7	+0.1	0.28	5	+0.2
N6340	Group center	1.05	3.12	2.11	> 15	-0.3	0.62	> 15	-0.3
N6548	Group member (pair)	1.91	4.71	3.02	(4)	(+0.5)	0	4	+0.5
N6654	Group member (pair)	1.36	4.19	2.68	(\geq 15)	(0)	0.24	15	0
N6703	Field	1.92	4.45	3.16	3	+0.6	0.38	3	+0.7
N7013	Field	2.09	3.30	2.35	3	+0.1	0.60	2	+0.2
N7280	Field	1.87	3.01	2.72	7	-0.1	0.07	7	-0.1
N7332	Field	1.60	2.66	2.14	(15)	(-0.3)	0.58	7	-0.2
N7457	Field	2.24	3.18	2.25	(4)	(-0.1)	0.20	4	-0.1
N7743	Field	2.18	3.00	2.47	(4)	(0)	1.48	< 2	+0.3
U11920	Field	1.78	4.06	2.80	(8)	(+0.2)	0.73	2	+0.5

^aGalaxy ID – N=NGC, U=UGC

^bFrom Guiricin et al. 2000

^cEstimated with the H β index corrected from the emission through the equivalent width of H α emission line

^dEstimated with the H β index corrected from the emission through the [OIII] λ 5007 equivalent width

Note. — The values of age and metallicity taken in parentheses are obtained without correcting the H β indices from emission

3. Stellar population properties in the nuclei and the bulges of S0s

Tables 4 and 5 contain the measured Lick indices $H\beta$, Mgb, and $\langle Fe \rangle \equiv (Fe5270 + Fe5335)/2$ for the nuclei and for the bulges correspondingly, as well as the parameters of the stellar population – luminosity-weighted age and metallicity – determined with these indices as described below. Some galaxies have measurements only for the nuclei or only for the bulges due to various reasons – for example, in NGC 5866 the nucleus is completely obscured by dust and in NGC 676 the bulge measurements are severely contaminated by a bright star projected at $5''$ from the nucleus. For the indices presented here, there are models based on evolutionary synthesis of simple (one-age, one-metallicity) stellar populations – see e.g. Worthey (1994). These models allow to estimate the luminosity-weighted mean metallicities and the ages of the stellar populations by confronting the hydrogen-line index $H\beta$ to any metal-line index. We are also going to consider the duration of the last major star-forming episode by confronting $\langle Fe \rangle$ to Mgb. Chemical evolution models, see e.g. Matteucci (1994), show that because of the difference in the timescales of iron and magnesium production by a stellar generation, the solar Mg/Fe abundance ratio can be obtained only by very continuous star formation, and brief star formation bursts, with $\tau \leq 0.1$ Gyr, would give significant magnesium overabundance, up to $[Mg/Fe] = +0.3 - +0.4$. In this work we use recent models by Thomas et al. (2003) because these models are calculated for several values of $[Mg/Fe]$: they allow to estimate Mg/Fe ratios of the stellar populations from Mgb and $\langle Fe \rangle \equiv (Fe5270 + Fe5335)/2$ measurements.

Figure 2 presents the $\langle Fe \rangle$ vs Mgb diagrams for the bulges and Fig. 3 – the similar diagrams for the nuclei, for all four types of environments. For some galaxies (e.g. NGC 2655 and NGC 2911) where the N $\lambda 5199$ emission is significant, the Mgb indices are corrected from this emission line according to the prescription of Goudfrooij & Emsellem (1996). The model sequences for $[Mg/Fe] = 0.0, +0.3, \text{ and } +0.5$ are well separated on the diagrams $\langle Fe \rangle$ vs Mgb, so we can estimate the mean Mg/Fe ratios ‘by eye’. Surprisingly, the bulges of the group central galaxies differ from those of the second-ranked group members: the former have the mean $[Mg/Fe] \approx +0.2$, and the latter – $+0.1$. As by the definition the second-rank group galaxies are less luminous than the central ones, this difference may be attributed not to the environment density, but to the galaxy mass effect, at the first glance. To check this, in Fig. 4 we have plotted the bulges only for the galaxies within the narrow stellar velocity dispersion range, $\sigma_* = 145 - 215$ km/s – in this σ_* range the central and second-rank group members of our sample have the same *mean* σ_* of 172 km/s; still the difference between the central group galaxies and the second-rank members persists in Fig. 4. This tendency of the S0s in the centers of groups to resemble more the cluster lenticulars, and of the second-rank group members and the paired galaxies to be like the field S0s, is in general confirmed by the nuclei distribution in the $\langle Fe \rangle$ vs Mgb diagrams (Fig. 3), though there are

more ‘outliers’ among the nuclei: evidently, the evolution of nuclear stellar populations bears more individual features than that of the bulges.

To break the age-metallicity degeneracy and to determine simultaneously the mean luminosity-weighted ages and the metallicities of the stellar populations, we confront the $H\beta$ indices to the combined metal-line index $[MgFe] \equiv (Mgb(Fe))^{1/2}$ – by plotting our data together with the models of Thomas et al. (2003); earlier we have assured that this diagram is insensitive to the Mg/Fe ratio. However we have one serious problem here: the absorption-line index $H\beta$ may be contaminated by emission, especially in the nuclear spectra. To correct from the emission the $H\beta$ indices which we have measured we have used data on equivalent widths of $H\alpha$ emission lines because $H\alpha$ emission lines are always much stronger than $H\beta$ emission lines and because an $H\alpha$ absorption line is not deeper than an $H\beta$ absorption line in spectra of stellar populations of any age while in intermediate-age population spectra it is much shallower. The emission-line intensity ratio, $H\alpha/H\beta$, has been studied well both empirically and theoretically. The minimum value of this ratio, 2.5, is known for the case of radiative excitation by young stars (Burgess 1958). For other types of excitation this ratio is higher. We have no pure H II-type nuclei in our sample, so here we use the formula $EW(H\beta_{emis}) = 0.25EW(H\alpha_{emis})$: this mean relation is obtained by Stasinska & Sodr e (2001) for a quite heterogeneous sample of nearby emission-line galaxies. The data on $EW(H\alpha_{emis})$ for the nuclei we take mainly from Ho et al. (1997). The bulge $H\beta$ indices were corrected from the emission by using $H\alpha$ equivalent widths obtained with the red MPFS spectra for about a half of the sample (28 objects, see the Table 1). Unlike Ho et al. (1997) who obtained $EW(H\alpha_{emis})$ by subtracting a pure absorption-line template from the observed spectra, we applied a multicomponent Gauss-analysis to the combinations of the $H\alpha$ absorption and emission lines which was effective due to mostly different velocity dispersions of stars and gas clouds in the galaxies under consideration. From the rest, 16 galaxies have negligible emission lines in the bulge spectra ($EW([O III]) \leq 0.3\text{\AA}$, see the Table 5), and for the others the age estimates obtained by using the $H\beta$ indices ‘corrected through the $H\alpha$ ’ (Table 5) are indeed only upper limits. To correct in some way ALL the bulge spectra, we have used also the wide-known approach which involves the $[O III]\lambda 5007$ emission line; Trager et al. (2000) recommend to use the statistical correction $\Delta H\beta = 0.6EW([OIII]\lambda 5007)$ though they note that individual ratios $H\beta/[O III]$ may vary between 0.33 and 1.25 within their sample of elliptical galaxies. In Fig. 5 we compare the corrections obtained by two different ways for the nuclei. If we exclude two galaxies with extremely strong emission in the centers – NGC 4138 and NGC 7743 – statistically the two types of the corrections are indistinguishable; however the accuracy of $[O III]$ measuring is not very high due to strong underlying absorption lines of Ti I, and the weak emission lines $[O III]$ with the equivalent widths of $EW \leq 0.3\text{\AA}$ are evidently artifacts. To summarize this analysis, we conclude that while for mutual

comparisons of the age distributions we must take only the age estimates corrected through the [O III] because this correction can be made for all galaxies of the sample, for the individual galaxies having the red spectra the estimates made with the $H\beta$ indices corrected through the $H\alpha$ are more reliable due to the facts that the $H\alpha$ emission is stronger and that the ratio of the Balmer emission lines depends only on the excitation mechanism unlike the ratio of $H\beta$ to [O III] which depends also on the metallicity of the gas.

Figure 6 presents the diagrams $H\beta$ vs [MgFe] for the nuclei (top) and for the bulges (bottom) of the galaxies of all types of environments with their $H\beta$ indices corrected through the $H\alpha$ to the left and with their $H\beta$ indices corrected through the [O III] to the right, correspondingly. By inspecting these diagrams, we determine the ages and the metallicities ‘by eye’ that provides an accuracy of ~ 0.1 dex in metallicity and 1 Gyr for the ages less than 8 Gyr and ~ 2 Gyr for older stellar systems which match our accuracy of the Lick indices. Directly in the diagrams one can see that the range of the ages of the nuclei is very wide: they may be as young as 1 Gyr old and as old as 15 Gyr old. The bulges are on average older than the nuclei, and in the bottom plots one can see a segregation of the galaxies according to their type of environment: most the bulges of the group centers and the cluster galaxies are older than 5 Gyr, whereas some of the group members and the field lenticulars have the bulges as young as 2-3 Gyr old. The metallicity ranges seem to be similar for the bulges in all types of environments: their [Z/H] are confined between ~ -0.3 and $\sim +0.4$. By fitting formally the metallicity distributions by Gaussians, we obtain the mean metallicity for the bulges in dense environments to be -0.04 and that for the bulges in sparse environments to be -0.13 , with the similar rms of 0.5 dex. The nuclei seem to be on average more metal-rich: only three nuclei in the galaxies of sparse environments have the metallicity less than the solar.

Kuntschner et al. (2002) have already reported the difference between the stellar population characteristics of the early-type galaxies in the dense and sparse environments. Their measurements were aperture spectroscopy, and their samples were the Fornax cluster as an example of dense environments and galaxies without more than 2 neighbors within the search radius of 1.3 Mpc as an example of sparse environments – the latter sample is probably close to our combination of the field plus paired galaxies. They have found that the E/S0 galaxies in sparse environments are younger than the E/S0 galaxies in the cluster by 2-3 Gyr – and our result for the S0s is quite the same. But they have also found the anti-correlation between the age and metallicity, the younger galaxies in sparse environments being on average more metal-rich (by 0.2 dex) than the older galaxies in the cluster; while if we see any metallicity difference, it should be in opposite sense.

In Fig. 7 we plot cumulative distributions of the ages: the number of galaxies not older

than T versus $\log T$ (in Gyr). We have united the samples of the brightest group S0s and the cluster galaxies into a ‘dense environment’ sample, and the group second-ranked members and the field S0s – into a ‘sparse environment’ sample. The effect of environments is seen both for the nuclei and for the bulges: in sparse environments the stellar populations are, on average, younger. The estimates of the median ages are the following: 3.7 and 6 Gyr for the nuclei of the galaxies in sparse and dense environments, correspondingly, and 4.8 and 8.3 Gyr for the bulges.

4. Discussion

It is a little bit surprising that according to my results, the ‘dense’ type of environment must be ascribed not only to the clusters but also to the centers of groups: the first-ranked and the second-ranked S0 galaxies of the groups have very different properties of their central stellar population. However, this conclusion is close to the recent finding by Proctor et al. (2004) that the early-type galaxies of Hickson compact groups resemble more the cluster galaxies than the field ones. I think it gives us a hint that the dynamical effect of close neighbors may play the main role in evolution rate, and not the mass of the common dark halo.

Table 6: The mean ages of the bulges within fixed stellar velocity dispersion ranges

Range of σ_* , km/s	Dense environments			Sparse environments		
	N_{gal}	$\langle T \rangle$, Gyr	Its rms	N_{gal}	$\langle T \rangle$, Gyr	Its rms
105–145	6	6.2 ± 2.2	4.9	6	4.5 ± 1.0	2.3
145–184	8	6.5 ± 1.0	2.6	9	6.6 ± 1.6	4.5
185–225	7	11.6 ± 1.2	2.8	5	8.6 ± 1.9	3.9

Recently some evidences have been published (Caldwell et al. 2003; Nelan et al. 2005) that the ages of the stellar populations in early-type galaxies are correlated with the central stellar velocity dispersion. In our sample, the galaxies in dense environments are on average more massive than those in sparse environments so one may suggest that the age difference found above may be due to the mass difference and not to the environment influence. To check this effect, I have plotted the bulge age estimates versus the central stellar velocity dispersion in Fig. 8. Indeed, the correlation is present implying that the more massive bulges are older; the slope of the regression $\log T$ vs $\log \sigma_{*,0}$ is 1.76 ± 0.65 for the dense environments and 1.30 ± 0.43 for the sparse ones with the correlation coefficients of 0.53 and 0.55, correspondingly. Following Caldwell et al. (2003), we have calculated the mean ages of the bulges within narrow ranges of stellar velocity dispersion (when the age estimate has only the low limit of 15 Gyr, I have ascribed the value of 16 Gyr to it). These estimates are given in Table 6 – please compare them with those in Caldwell et al. (2003), 7.4 Gyr, rms 4.2 Gyr, in the range of $\sigma_* = 100 - 160$ km/s, and 9.9 Gyr, rms 4.2 Gyr, in the range of $\sigma_* > 160$ km/s. One can see from Table 6 that the ages of the bulges are the same in different types of environments for the lower bins of σ_* , 105–145 and 145–185 km/s; but in the highest bin, 185–225 km/s, the ages are dramatically different, the massive bulges in dense environments being much older than the massive bulges in sparse environments. By inspecting Fig. 8, we notice that the separation between the bulges in different types of environments starts from about $\sigma_* = 170$ km/s. Taking 7 galaxies in dense environments and 7 galaxies in sparse environments with the σ_* in the range of 170–215 km/s, we obtain $\langle T \rangle = 9.7 \pm 1.3$ Gyr, rms 3.2 Gyr, for the former and $\langle T \rangle = 6.6 \pm 1.5$ Gyr, rms 3.7 Gyr, for the latter subsample; so the difference is 3.1 ± 2.0 Gyr. The application of the Student T-statistics to this double subsample of the massive bulges shows that the mean age of the massive bulges in dense environments is larger than the mean age of the massive bulges in sparse environments with the probability higher than 0.85 (the hypothesis of $\langle T \rangle_{\text{dense}} \leq \langle T \rangle_{\text{sparse}}$ is rejected at the significance level of 0.14).

5. Conclusions

By considering the stellar population properties in the nuclei and the bulges of the nearby lenticular galaxies in the various types of environments, I have found certain differences between the nuclei and the bulges as well as between the galaxies in dense and sparse environments. The nuclei are on average younger than the bulges in any types of environments, and both the nuclei and the bulges of S0s in sparse environments are younger than those in dense environments. The results of the consideration of the Mg/Fe ratios suggest that the main star formation epoch may be more brief in the centers of the galaxies in dense

environments.

I am grateful to the astronomers of the Special Astrophysical Observatory of RAS V.L. Afanasiev, A.N. Burenkov, V.V.Vlasyuk, S.N. Dodonov, and A.V. Moiseev for supporting the MPFS observations at the 6m telescope. The 6m telescope is operated under the financial support of Science Ministry of Russia (registration number 01-43); we thank also the Programme Committee of the 6m telescope for allocating the observational time. During the data analysis we have used the Lyon-Meudon Extragalactic Database (LEDA) supplied by the LEDA team at the CRAL-Observatoire de Lyon (France) and the NASA/IPAC Extragalactic Database (NED) which is operated by the Jet Propulsion Laboratory, California Institute of Technology, under contract with the National Aeronautics and Space Administration. The study of the young nuclei in lenticular galaxies was supported by the grant of the Russian Foundation for Basic Researches no. 01-02-16767.

REFERENCES

- Afanasiev, V.L., Sil'chenko, O.K. 2000, AJ, 119, 126
- Afanasiev, V.L., Sil'chenko, O.K. 2002, AJ, 124, 706
- Afanasiev, V.L., Dodonov, S.N., Moiseev, A.V., 2001, In: Stellar dynamics: from classic to modern/ Eds. Osipkov L.P. and Nikiforov I.I., Saint Petersburg Univ. press, 103
- Bacon, R., Adam, G., Baranne, A., Courtes, G., Bubet, D., et al. 1995, A&AS, 113, 347
- Burgess, A., 1958, MNRAS, 118, 477
- Byrd, G., Valtonen, M., 1990, ApJ, 350, 89
- Caldwell, N., Rose, J.A., Concannon, K.D. 2003, AJ, 125, 2891
- De Lucia, G., Springel, V., White, S.D.M., Croton, D., Kauffmann, G. 2005, MNRAS, in press, astro-ph/0509725
- Fasano, G., Poggianti, B.M., Couch, W.J., Bettoni, D., Kjaergaard, P., Moles, M., 2000, ApJ, 542, 673
- Giuricin, G., Marinoni, C., Ceriani, L., Pisani, A. 2000, ApJ, 543, 178
- Goto, T., Okamura, S., Sekiguchi, M., Bernardi, M., Brinkmann, J., et al. 2003, PASJ, 55, 757
- Goudfrooij, P., Emsellem, E. 1996, A&A, 306, L45
- Ho, L.C., Filippenko, A., Sargent, W.L. 1997, ApJS, 112, 315
- Hubble, E.P., 1936, Realm of the Nebulae, Yale Univ. Press
- Kochanek, C.S., Falco, E.E., Impey, C.D., Lehár, J., McLeod, B.A., et al., 2000, ApJ, 543, 131, 2000
- Kuntschner, H., Smith, R.J., Colless, M., Davies, R.L., Kaldare, R., Vazdekis, A. 2002, MNRAS, 337, 172
- Lanzoni, B., Guiderdoni, B., Mamon, G.A., Devriendt, J., Hatton, S. 2005, MNRAS, 361, 369
- Larson, R.B., Tinsley, B.M., Caldwell, C.N. 1980, ApJ, 237, 692

- Matteucci, F. 1994, *A&A*, 288, 57
- Moore, B., Katz, N., Lake, G., Dressler, A., Oemler, A., Jr., 1996, *Nature*, 379, 613
- Nelan, J.E., Smith, R.J., Hudson, M.J., Wegner, G.A., Lucey, J.R., et al. 2005, *ApJ*, 632, 137
- Proctor, R.N., Forbes, D.A., Hau, G.K.T., Beasley, M.A., De Silva, et al., 2004, *MNRAS*, 349, 1381
- Quilis, V., Moore, B., Bower, R., 2000, *Science*, 288, 1617
- Sil'chenko, O.K. 1993, *Pis'ma v AZh*, 19, 701
- Sil'chenko, O.K. 1998, *A&A*, 330, 412
- Sil'chenko, O.K. 1999, *AJ*, 117, 2725
- Sil'chenko, O.K. 2000, *AJ*, 120, 741
- Sil'chenko, O.K., Vlasyuk V.V. 2001, *Pis'ma v AZh*, 27, 19
- Sil'chenko, O.K., Afanasiev, V.L. 2002, *A&A*, 385, 1
- Sil'chenko, O.K., Afanasiev, V.L. 2004, *AJ*, 127, 2641
- Sil'chenko, O.K., Afanasiev V.L., Chavushyan, V.H., Valdes, J.R. 2002, *ApJ*, 577, 668
- Sil'chenko, O.K., Moiseev, A.V., Afanasiev, V.L., Chavushyan, V.H., Valdes, J.R. 2003, *ApJ*, 591, 185
- Sil'chenko, O.K., Kuposov, S.E., Vlasyuk, V.V., Spiridonova, O.I. 2003, *Astronomy Reports*, 47, 88
- Stasinska, G., Sodré, I., Jr. 2001, *A&A*, 374, 919
- Terlevich, A.I., Forbes, D.A. 2002, *MNRAS*, 330, 547
- Thomas, D., Maraston, C., Bender, R. 2003, *MNRAS*, 339, 897
- Thomas, D., Maraston, C., Bender, R., Mendes de Oliveira, C., 2005, *ApJ*, 621, 673
- Trager, S.C., Worthey, G., Faber, S.M., Burstein, D., González, J.J. 1998, *ApJS*, 116, 1
- Trager, S.C., Faber, S.M., Worthey, G., González, J.J. 2000, *AJ*, 119, 1645

Tully, R.B., Verheijen, M.A.W., Pierce, M.J., Huang, J.-S., Wainscoat, R.J. 1996, *AJ*, 112, 2471

Worthey, G. 1994, *ApJS*, 95, 107

Worthey, G., Faber, S.M., González, J.J., Burstein, D. 1994, *ApJS*, 94, 687

Yamauchi, Ch., Goto, T. 2004, *MNRAS*, 352, 815

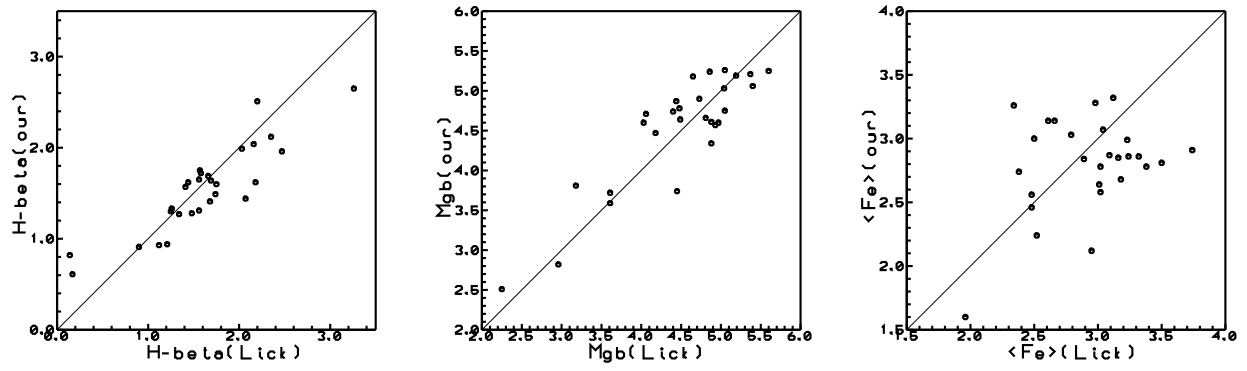


Fig. 1.— The comparison of our measurements of the nuclear Lick indices with the aperture data of Trager et al. (1998) for 28 common galaxies. The straight lines are the bissectrices of the quadrants ('the lines of equality')

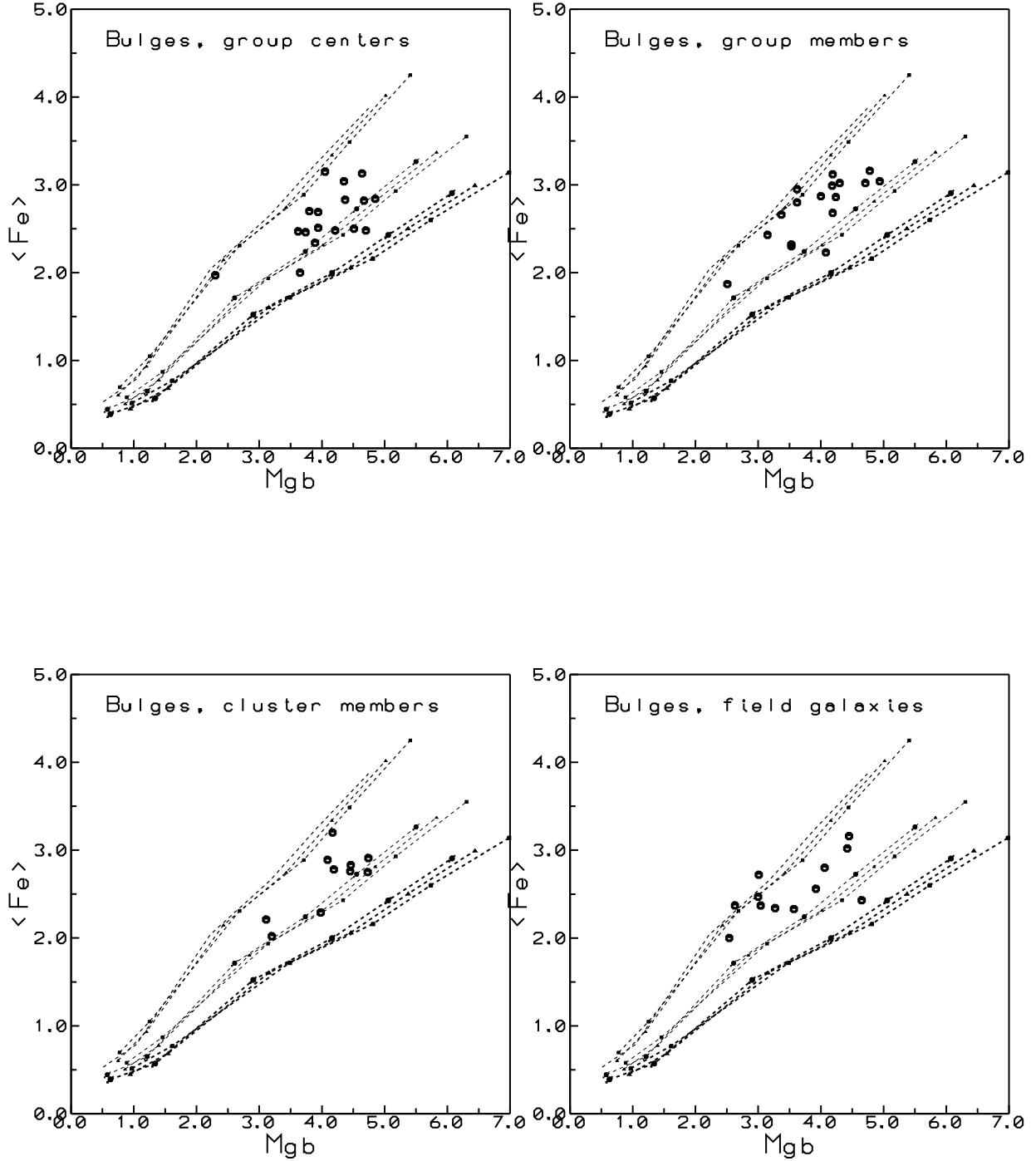


Fig. 2.— The $\langle \text{Fe} \rangle$ vs Mgb diagrams for the bulge index measurements. The typical accuracy of the azimuthally averaged indices is 0.1 \AA – 0.15 \AA . The simple stellar population models of Thomas et al.(2003) for three different magnesium-to-iron ratios (0.0, +0.3, and +0.5, if the curve triads are taken from top to bottom) and three different ages (5, 8, and 12 Gyr from top to bottom in every triad) are plotted as reference. The small signs along the model curves mark the metallicities of +0.67, +0.35, 0.00, -0.33, -1.35, and -2.25, if one takes the signs from right to left.

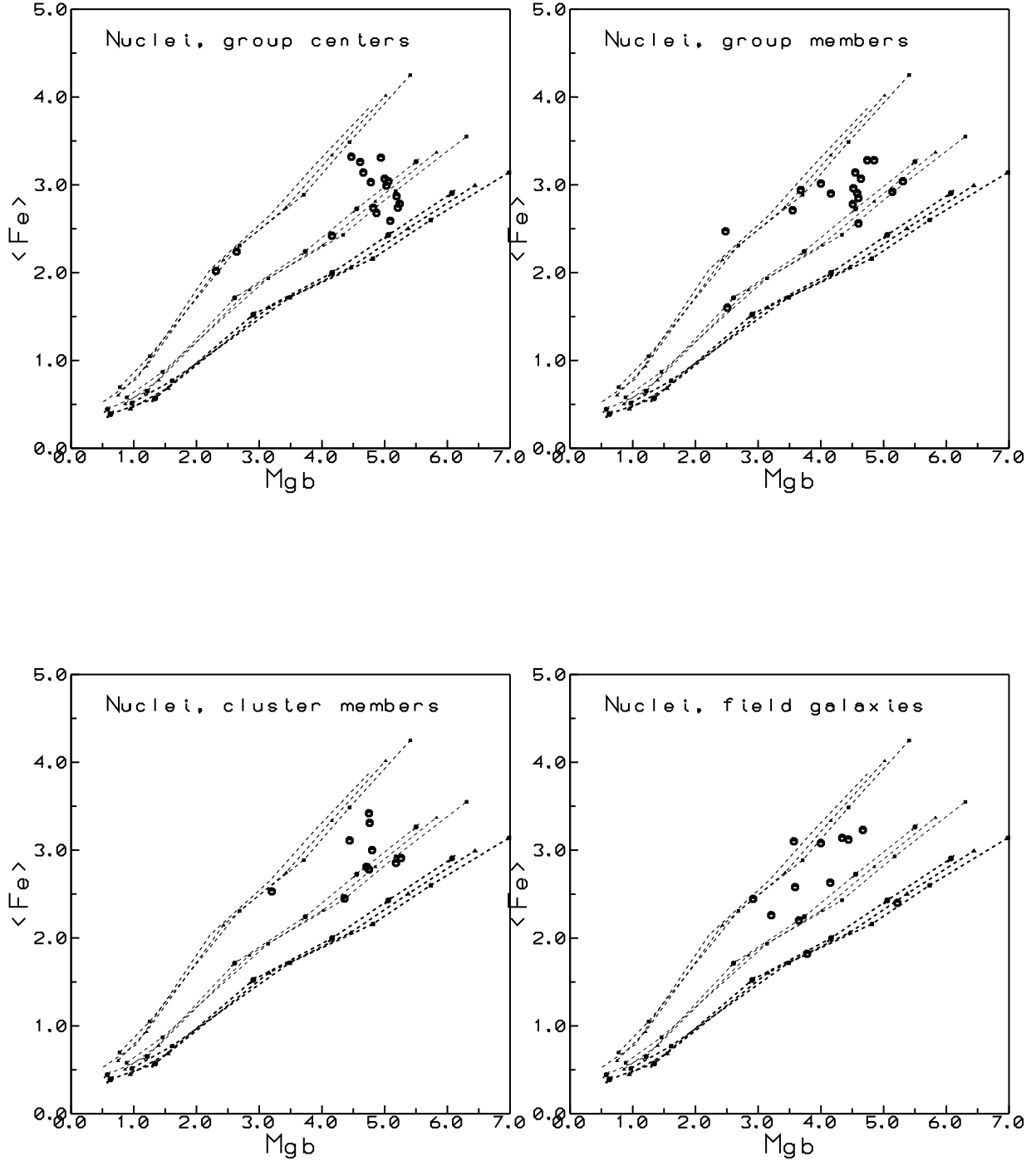


Fig. 3.— The $\langle \text{Fe} \rangle$ vs Mgb diagrams for the nucleus index measurements. The typical accuracy of the nuclear indices is 0.1 \AA – 0.15 \AA . The simple stellar population models of Thomas et al.(2003) for three different magnesium-to-iron ratios (0.0, +0.3, and +0.5, if the curve triads are taken from top to bottom) and three different ages (5, 8, and 12 Gyr from top to bottom in every triad) are plotted as reference. The small signs along the model curves mark the metallicities of +0.67, +0.35, 0.00, -0.33, -1.35, and -2.25, if one takes the signs from right to left.

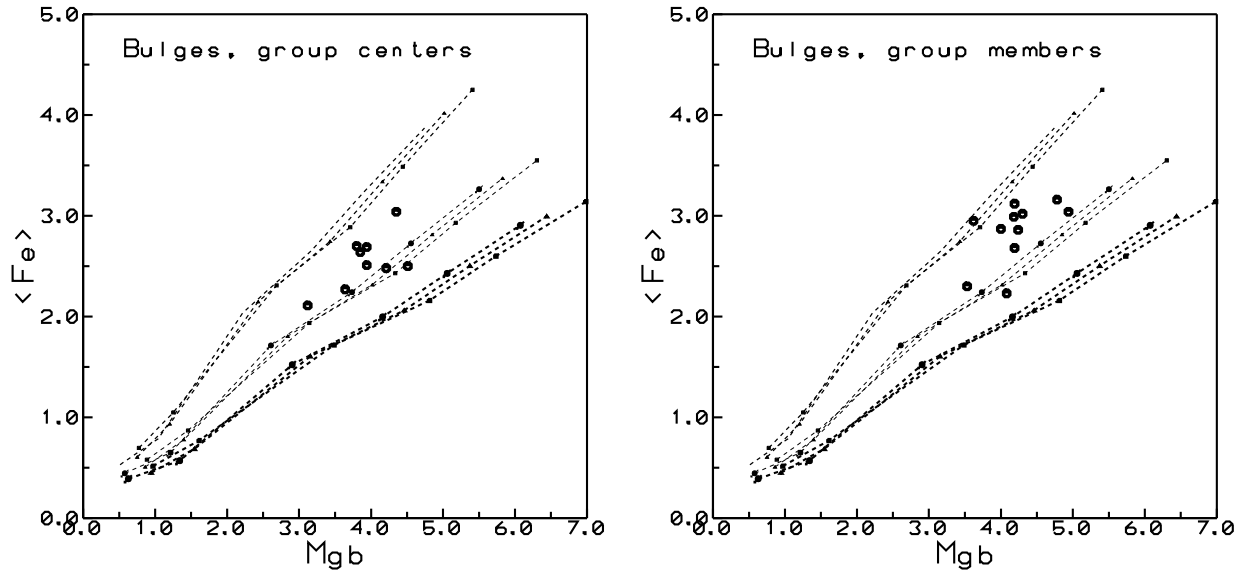


Fig. 4.— The same as in Fig. 2, but only for the group galaxies with σ_* within the range of 145–215 km/s

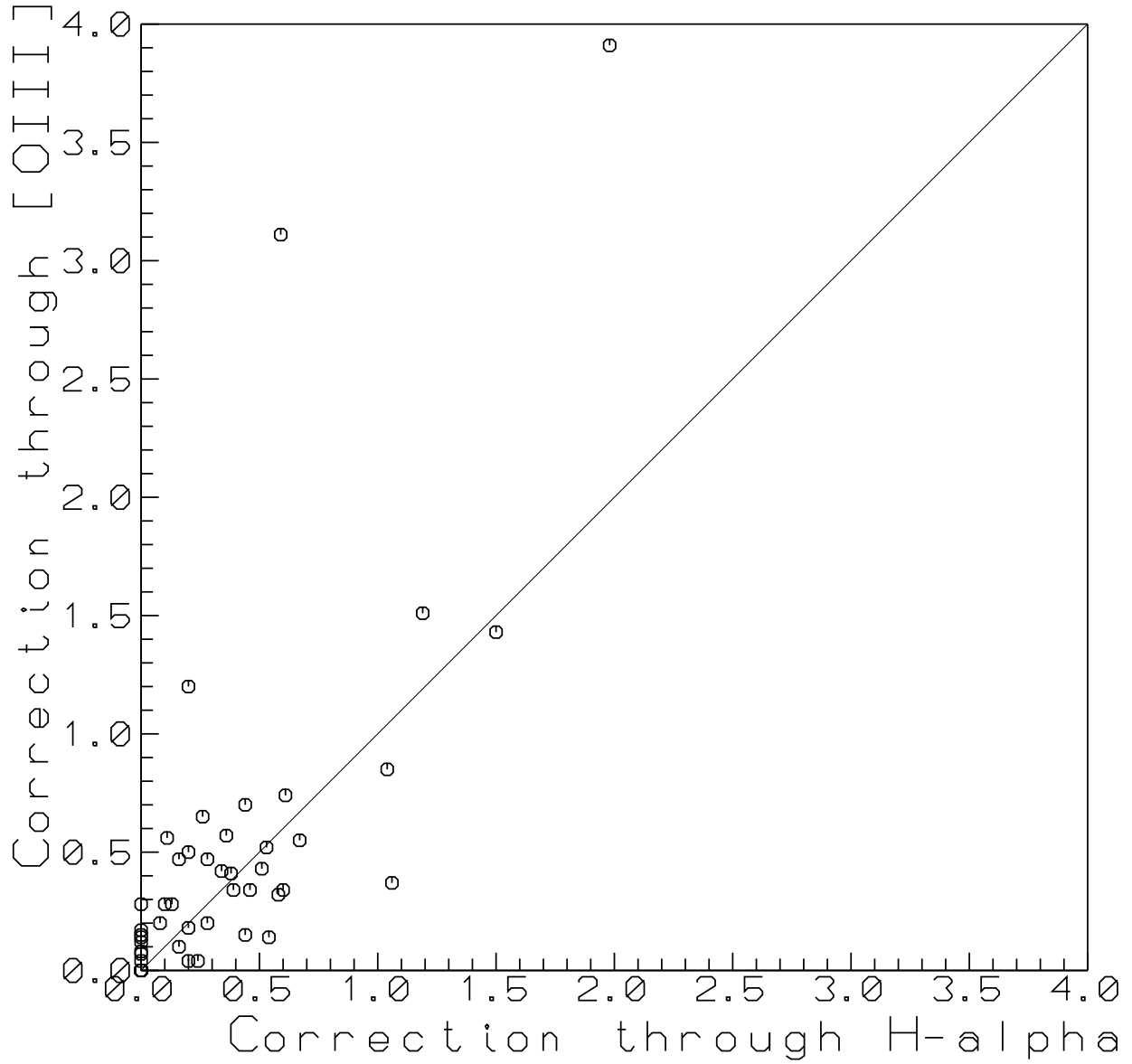


Fig. 5.— The comparison of the $H\beta$ index corrections from the emission obtained by two different ways – through $H\alpha$ equivalent widths and through [O III] equivalent widths as described in the text. The straight line is the bisectrice of the quadrant ('the line of equality')

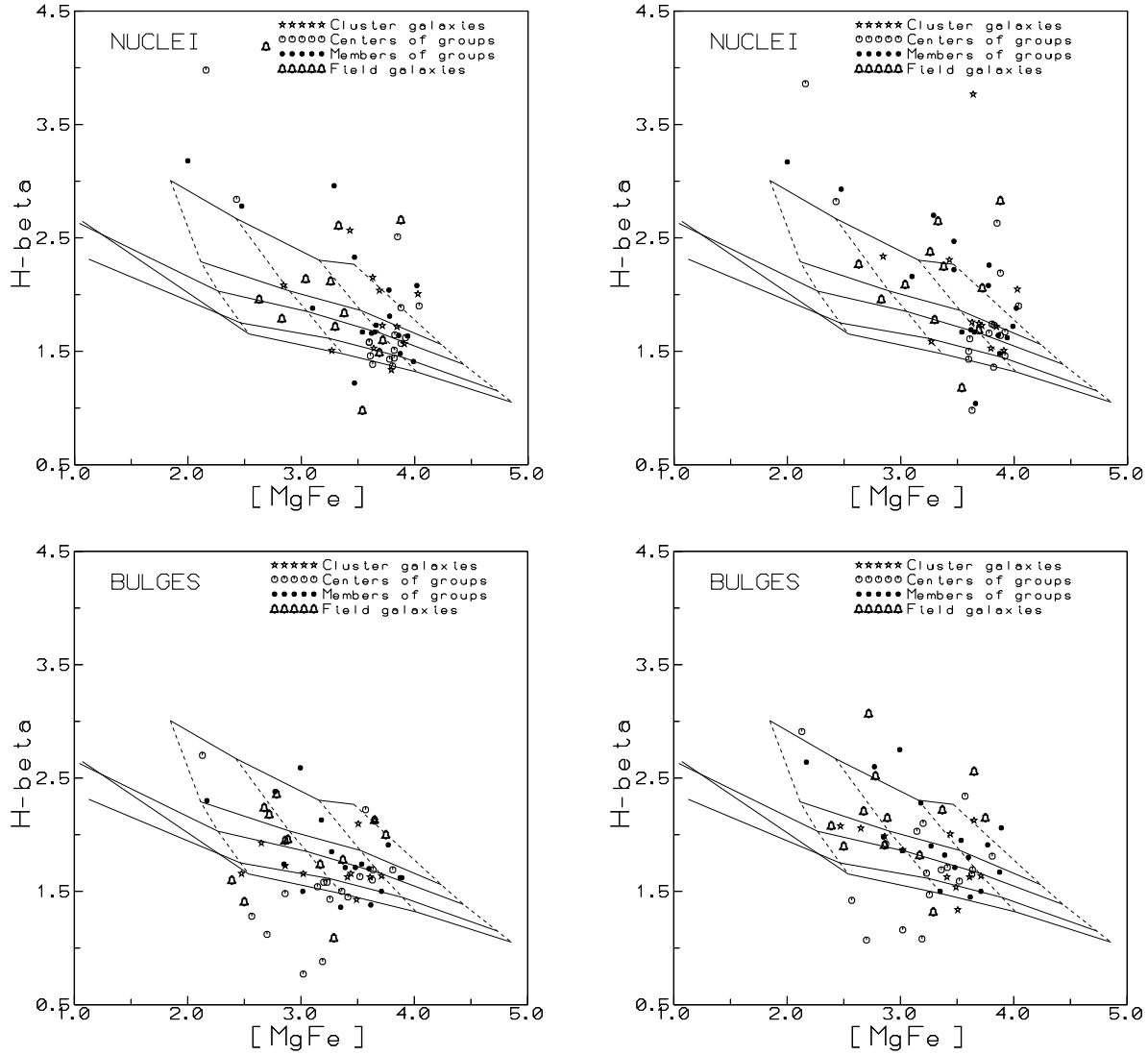


Fig. 6.— The age-diagnostic diagrams for the stellar populations in the nuclei (*top*) and circumnuclear regions (*bottom*) of the galaxies under consideration; the $H\beta$ -index measurements are corrected from the emission contamination by using $H\alpha$ in the left plots and by using [O III] in the right plots, as described in the text. The typical accuracy of the indices is 0.1 \AA for the combined metal-line index and 0.15 \AA for the $H\beta$. The stellar population models of Thomas et al.(2003) for $[Mg/Fe]= +0.3$ and five different ages (2, 5, 8, 12, and 15 Gyr, from top to bottom curves) are plotted as reference frame; the dashed lines crossing the model curves mark the metallicities of +0.67, +0.35, 0.00, -0.33 from right to left. In the top right plot the nucleus of NGC 7743 which has $H\beta_{\text{corr}} > 6 \text{ \AA}$ is omitted.

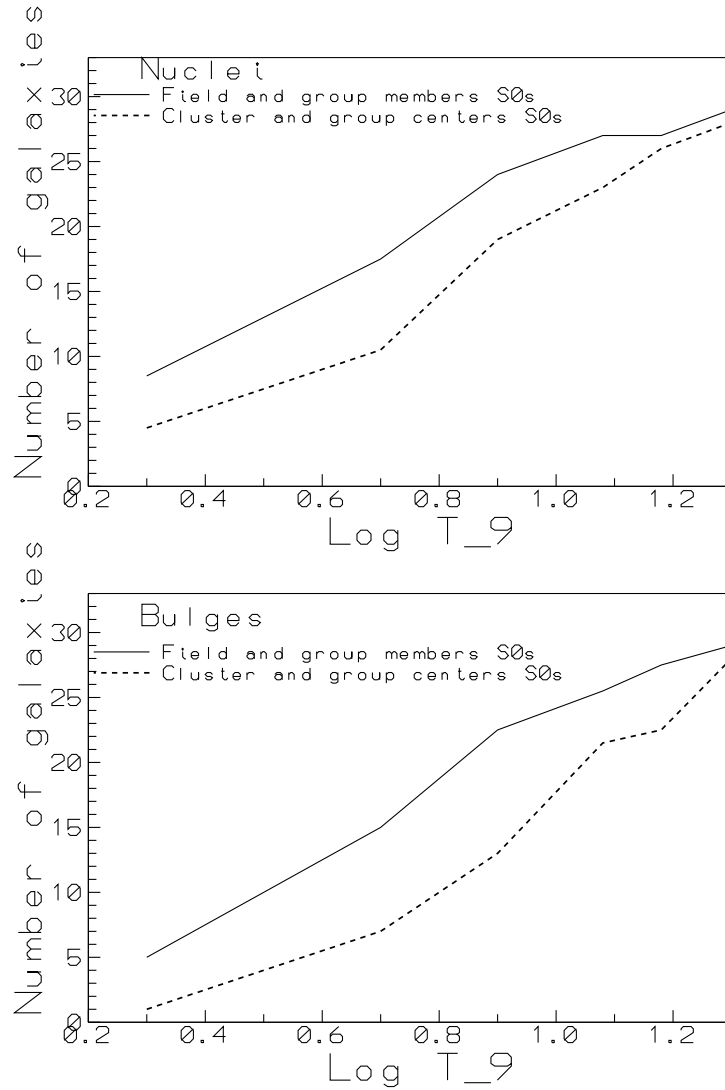


Fig. 7.— Cumulative age distributions: the number of objects younger than abscissa which is $\log T$ in Gyr vs $\log T$. (a) The stellar nuclei of the galaxies (b) The bulges taken in the rings between $R = 4''$ and $R = 7''$.

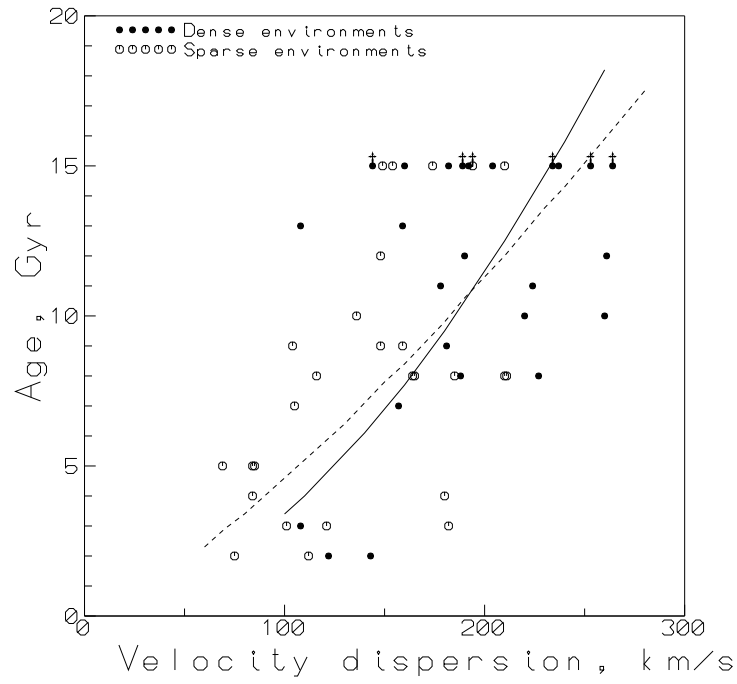


Fig. 8.— Relation between the bulge age estimates obtained in this work and central stellar velocity dispersions: the regression straight lines fitting the dependencies of $\log T$ on $\log \sigma$ are converted into linear units and plotted by a solid line for the dense environment galaxies and by a dashed line for the sparse environment galaxies